

Striped spin liquid crystal ground state instability of kagome antiferromagnets

Bryan K. Clark,^{1,2,*} Jesse M. Kinder,^{3,4,*} Eric Neuscamman,^{5,4} Garnet Kin-Lic Chan,^{6,4} and Michael J. Lawler^{7,8,†}

¹Station Q, Microsoft Research, Santa Barbara, CA 93106, USA

²Princeton University and Princeton Center for Theoretical Science, Department of Physics, Princeton, NJ 08544

³Case Western Reserve University, Department of Physics, Cleveland, OH 44106

⁴Cornell University, Department of Chemistry, Ithaca, NY 14853

⁵University of California Berkeley, Department of Chemistry, Berkeley, CA 94720

⁶Princeton University, Department of Chemistry, Princeton, NJ 08544

⁷Department of Physics, Binghamton University, Binghamton, NY 13902-6000

⁸Department of Physics, Cornell University, Ithaca, NY 14853

(Dated: November 20, 2021)

The Dirac spin liquid ground state of the spin 1/2 Heisenberg kagome antiferromagnet has potential instabilities [1–4]. This has been suggested as the reason why it is not strongly supported in large-scale numerical calculations[5]. However, previous attempts to observe these instabilities have failed. We report on the discovery of a projected BCS state with lower energy than the projected Dirac spin liquid state which provides new insight into the stability of the ground state of the kagome antiferromagnet. The new state has three remarkable features. First, it breaks both spatial symmetry in an unusual way that may leave spinons deconfined along one direction. Second, it breaks the $U(1)$ gauge symmetry down to Z_2 . Third, it has the spatial symmetry of a previously proposed “monopole” suggesting that it is an instability of the Dirac spin liquid. The state described herein also shares a remarkable similarity to the distortion of the kagome lattice observed at low Zn concentrations in Zn-Paratacamite suggesting it may already be realized in these materials.

Many potential ground states have been suggested for the spin 1/2 kagome Heisenberg antiferromagnet; these include magnetic ordering in one of several spin patterns[6], a valence bond crystal with a 36 site unit cell[7] or a 12 site unit cell[5], a chiral spin liquid[7, 8], several kinds of Z_2 spin liquids[9, 10] and an algebraic spin liquid[1, 3]. Amongst algebraic spin liquids, it was shown [3] that the $U(1)$ -Dirac state had lowest variational energy. This latter state is characterized by its graphene-like Dirac fermionic spinons interacting with a Maxwell-like photon that characterizes singlet excitations. Many of the other suggestions for the kagome antiferromagnet ground state can be characterized as instabilities of this Dirac spin liquid; these instabilities have been catalogued in ref. 4. However, despite the many instabilities, all variational studies we are aware of that include the $U(1)$ -Dirac state for some choice of variational parameters have found it remarkably stable[2–4, 11, 12].

Recently, large scale DMRG calculations[5, 13, 14] have produced strong numerical evidence that the true ground state of the kagome antiferromagnet is a Z_2 spin liquid. In particular, they have found the lowest known variational state with energies comparable to exact diagonalization on small clusters, a gap to all excitations and topological entanglement entropy expected of a Z_2 spin liquid. These results are quite surprising in light of prior studies of the $U(1)$ -Dirac state and suggest that it is unstable.

Perhaps the simplest explanation of the DMRG results,

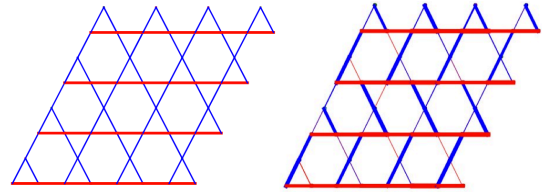


FIG. 1. The n.n. $\vec{s}_i \cdot \vec{s}_j$ correlations for the projected Dirac Spin liquid state with twisted boundary conditions (left) and the lowest energy projected mean field state (right). The color indicates sign and the linewidth measures the magnitude.

as proposed in Ref. 10, is that the Dirac-like spinons pair up and form a superfluid-like Z_2 spin liquid. With this goal in mind, these authors catalog 20 such possible states and give explicit instructions for constructing 14 of them. Unfortunately, despite searches for such a state[12], no Z_2 state has been shown to be energetically favorable to the $U(1)$ Dirac state at the level of variational projected BCS wave functions.

In this letter, we revisit the projected BCS (PBCS) variational wave function problem on the kagome lattice and have discovered an instability of the Dirac state. Our approach, building on Refs. 15 and 16, is to optimize over the entire set of time-reversal invariant projected BCS wave functions which are parameterized by a symmetric pairing matrix ϕ_{ij} . These states encompass the $U(1)$ and Z_2 spin liquids, general valence bond solids, and a number of other instabilities. We find states with lower energy than the Dirac state on clusters of up to 192 sites. On the 48 site cluster in particular, a carefully optimized wave function, as shown in Fig. 1, demonstrates

* These authors contributed equally.

† mlawler@binghamton.edu

that the new state breaks lattice symmetries, doubling the unit cell with a wave vector that connects the two Dirac nodes. However it preserves a C_2 rotational symmetry about several lattice points giving it a distinct one dimensional character. It also lies very close to the Dirac state with similar fluxes through the hexagons and bow ties. For these reasons, we believe it should belong to one of the leading instabilities proposed in Ref. 4, and have discovered that the most likely candidate is the time-reversal symmetric “ w -monopole”. We also find that this state cannot be obtained by optimizing within the class of wave functions that do not admit pairing and therefore likely has Z_2 global gauge symmetry. For this reason and because of its C_2 symmetry and one dimensional character, we have dubbed this state a Z_2 striped (or smectic) spin liquid crystal. Finally, we discuss a connection between our state and Zn-Paratacamite with Zn concentrations x below $x = 1/3$ whose observed distorted kagome layers[17] has the same symmetry as Fig. 1(b).

Our objective is to find the ground state of the nearest neighbor spin 1/2 kagome antiferromagnet constrained to the set of Gutzwiller projected variational BCS wave functions

$$|\Psi\rangle = \hat{\mathcal{P}}_{S=1/2}|\Psi_0\rangle \quad (1)$$

where $\Psi_0(R) = \langle R|\Psi_0\rangle = \det M(R)$, $M_{ij}(R) = \phi(\vec{r}_{i\uparrow}, \vec{r}_{j\downarrow})$ is the BCS pairing amplitude and $\hat{\mathcal{P}}_{S=1/2}$ projects these states onto the physical singly occupied Hilbert space of spin wave functions. This set of variational ansatz includes projected Slater determinants such as the $U(1)$ Dirac spin liquid [3]. The variational search is performed by minimizing the ground state energy

$$E = \langle \Psi | \hat{H} | \Psi \rangle, \quad \hat{H} = \sum_{\langle ij \rangle} \hat{S}_i^\alpha \hat{S}_j^\alpha. \quad (2)$$

of the Heisenberg spin Hamiltonian on the kagome lattice using as parameters all $n(n-1)/2$ real values of the pairing function $\phi(\vec{r}_i, \vec{r}_j)$ (building on Refs. 15 and 16). To avoid only finding local minima in this energy landscape, we choose to start the optimization in many qualitatively different starting points by making use of the well developed projective symmetry group classification developed in the literature[3, 4, 10, 18]. In particular, we will choose mean field parameters following Ref. 10 and derive a pairing matrix from these following supplemental materials(SM) S-I and S-II. This allows us to start from 14 different spin liquid wave functions. Fig. 2(a) shows prototypical optimization traces of the energies for each spin liquid state on the 4×4 lattice, labeled following Table II of Ref. 10. Many states lie below the energy of the Dirac spin liquid and the minimal energy state we find is at $-0.430520 \pm 5 \times 10^{-6}$ per site (see SM S-III for its pairing matrix), significantly below the Dirac spin liquid energy of $0.42938 \pm 4 \times 10^{-5}$ per site showing that the Dirac spin liquid is not the most stable projected mean field state.

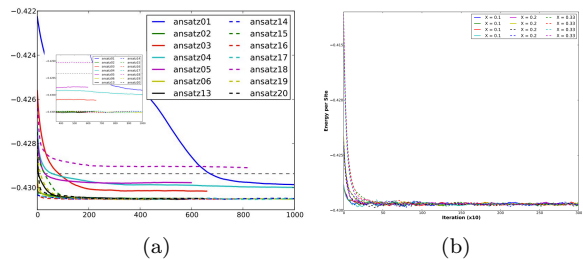


FIG. 2. (a): Prototypical stochastic optimization traces starting from the 14 distinct PSG ansatz defined in Table II of Ref. 10 and optimizing the pairing function ϕ . Inset shows magnified version. (b): Optimization of only single particle orbitals starting from perturbed Dirac states where X labels the strength of the perturbation.

This is particularly surprising in light of previous studies that find the Dirac spin liquid to be stable against many instabilities[1, 3, 4, 12, 19]. Such calculations failed to find this state because they only considered short-range mean field Hamiltonians, a limitation we avoid by optimizing a general pairing function that allows both long-range hopping terms and spatial symmetry breaking in the fermion Hamiltonian. As shown in Fig. 2(b) and discussed in more detail below, our approach in conjunction with enforcing $U(1)$ symmetry does not lower the energy. But, additionally allowing the $U(1)$ gauge symmetry to break down to Z_2 does lower the energy (left side of Fig. 2). Consequently, the gauge symmetry breaking down to Z_2 is intricately linked to spatial symmetry breaking and also possibly long-range hopping/pairing terms in the Hamiltonian.

Let us then focus on the nature of our lowest energy state. Most strikingly we find that the state breaks translational symmetry doubling the unit cell. Fig. 1 (right) shows the deviation of the spin-spin correlation function on nearest neighbors from its average value, in contrast with the $U(1)$ Dirac spin liquid shown in Fig. 1 (left). The symmetry breaking seen in the Dirac spin liquid is a finite size artifact coming from twisted boundary conditions in one direction. In our optimized state we find breaking of the translational symmetry and a doubling of the unit cell leading us to conclude that the minimal projected mean field state is *not* an isotropic spin liquid.

To further verify that there is not a nearby isotropic spin liquid state to our optimal state, we stochastically modify the pairing function, starting from a low energy state, in small increments searching for a true symmetric spin liquid. In particular, we make a random stochastic change to the pairing function accepting it only if we have moved closer to a spin liquid state (defined by the deviations of the unprojected $\langle \vec{S}_i \cdot \vec{S}_j \rangle$). In this way, we search for the “closest” spin liquid. When we run this procedure, the spin liquid state it approaches has the energy of the Dirac spin liquid (and hence is presumably

the Dirac spin liquid). This leads us to believe that their is no additional nearby isotropic spin liquid.

Having found a broken symmetry state, we would like to now understand whether it retains characteristics reminiscent of any spin liquid phase. To make such a connection, it is useful to compute the anomalous density matrix from the unprojected wave function defined by the pairing matrix that corresponds to our lowest energy projected state. It is given by

$$\rho_{ij} = \begin{pmatrix} -A_{ij}^* & B_{ij} \\ B_{ij}^* & A_{ij} \end{pmatrix} \quad (3)$$

where

$$A_{ij} = \frac{\langle \Psi_0 | f_{i\downarrow}^\dagger f_{j\downarrow} | \Psi_0 \rangle}{\langle \Psi_0 | \Psi_0 \rangle}, \quad B_{ij} = \frac{\langle \Psi_0 | f_{i\uparrow}^\dagger f_{j\downarrow} | \Psi_0 \rangle}{\langle \Psi_0 | \Psi_0 \rangle} \quad (4)$$

and transforms under an $SU(2)$ gauge transformation, $\Psi \rightarrow \mathbf{G} \cdot \Psi$, like $\rho_{ij} \rightarrow \mathbf{G}_i \cdot \rho_{ij} \cdot \mathbf{G}_j^\dagger$ exactly like the mean fields in the corresponding slave particle theory (see Ref. [20] or the SM S-I). We can therefore use this matrix to study the projective symmetry properties of the obtained unprojected state $|\Psi_0\rangle$.

To study fluxes through the lattice, we can use the $SU(2)$ matrix version of a ‘‘phase’’ variable

$$\mathbf{W}_{ij} = -i\rho_{ij}/|\rho_{ij}| \quad (5)$$

that is an analog of the $U(1)$ phase $e^{ia_{ij}}$ we associate with ordinary electricity and magnetism on a lattice. Following Ref. 20, the analog of flux through any loop on the lattice is therefore the product of this matrix around the loop

$$\Phi_{ijk\dots l} = i^{N_{loop}} \mathbf{W}_{ij} \cdot \mathbf{W}_{jk} \cdot \dots \cdot \mathbf{W}_{li} \quad (6)$$

where N_{loop} is the number of bonds ij that form the loop. Unfortunately, this product is not gauge invariant, but for every loop of the lattice, we can define an angle θ associated with its flux through the trace of this matrix. Unlike a $U(1)$ flux, here $\theta = 2\pi$ introduces a phase change of -1 . The natural first loops to consider when characterizing the state $|\Omega\rangle$ are the nearest neighbor bow ties (product of two neighboring triangles) and hexagons (the trace of $\Phi_{ijk\dots l}$ for an odd site loop vanishes by time reversal symmetry). These loops allow us to determine which of the four $U(1)$ spin liquid states is closest to our best optimized state. The results are

$$\langle \theta_{\text{hex}} \rangle = (1.994 \pm 0.003)\pi, \quad \langle \theta_{\text{bow}} \rangle = (0.010 \pm .007)\pi \quad (7)$$

where the error estimate is the standard deviation and $\langle \dots \rangle$ denotes the average value of the flux over different hexagons or bow ties respectively. These results are equivalent to nearly π flux through the hexagon and 0 flux through the bow tie or triangle in the traditional $U(1)$ description of flux. They show distinctly that the

optimized state is very close to the $U(1)$ Dirac state as expected from energetic considerations but that because of the symmetry breaking shown in Fig. 1 it is an instability.

Having established that our newly discovered state is very close to the Dirac state, we now turn to its symmetry breaking properties. To this end, we seek the space group representations that give the largest contribution to the pattern in Fig. 1(b) which are periodic with at most a quadrupled unit cell. Such representations were constructed in Ref. [4] and labeled as $A_1, A_2, B_1, B_2, E_1, E_2$ for those related to the point group alone and $F_1, F_2 = F_1 \otimes A_2, F_3 = F_1 \otimes B_1, F_4 = F_1 \otimes B_2$ for those allowed by a doubling/quadrupling of the unit cell. The focus of Ref. [4] was on the F_1 representation for the ‘‘Hastings valence bond crystal’’ states associated with the generation of mass of the Dirac fermions. However, the bond amplitudes plotted in Fig. 1(b) are not of this representation. Instead, they are dominated by the F_2 and E_2 representations whose patterns are shown in Fig. 3 (a) and (b). Remarkably, the symmetry of the F_2 pattern alone is the same as the symmetry of the F_2 and E_2 patterns. The E_2 pattern alone, however, has higher symmetry. Hence, the symmetry breaking observed here arises uniquely from a desire to form the F_2 pattern.

The only time reversal symmetric alternative to the Hastings states, among instabilities of the Dirac fixed point identified in Ref. [4] is the spin singlet/nodal triplet ‘‘ w -monopole’’ that is created by a complex operator $w_i, i = x, y, z$ [4]. In SM S-IV we show, following the transformation properties determined in Ref. [4], that the six dimensional vector $(\text{Re } w_x, \text{Re } w_y, \text{Re } w_z, \text{Im } w_x, \text{Im } w_y, \text{Im } w_z)^T$ transforms under the two three-dimensional representations F_1 and F_2 . This remarkable coincidence allows us to conjecture that the w -monopole is responsible for the instability of the Dirac state observed in Fig. 1(b).

To further understand the role of the symmetry breaking, we measure the asymmetry of Fig. 1 during part of an optimization run and correlate this with the observed energy. We compare global asymmetry (removing the E_2 representation to remove the effects of twisted boundary conditions) defined as

$$\mathcal{O} = \sum_{\langle ij \rangle} \langle \Psi_0 | \vec{S}_i \cdot \vec{S}_j | \Psi_0 \rangle - E_{2ij}^1 \langle \Psi_0 | \vec{S}_i \cdot \vec{S}_j | \Psi_0 \rangle \quad (8)$$

as well as the asymmetry of the F_2 component defined as

$$\mathcal{O}_{F_2} = \sum_{\langle ij \rangle} F_{2ij}^1 \langle \Psi_0 | \vec{S}_i \cdot \vec{S}_j | \Psi_0 \rangle \quad (9)$$

where $F_{2ij}^1 = 1/\sqrt{2N_b/3}$ on the solid thick bonds, $F_{2ij}^1 = -1/\sqrt{2N_b/3}$ on the dashed thick bonds and zero otherwise with N_b the number of nearest neighbor bonds. These are shown in Fig. 3 (c) and (d). Interestingly,

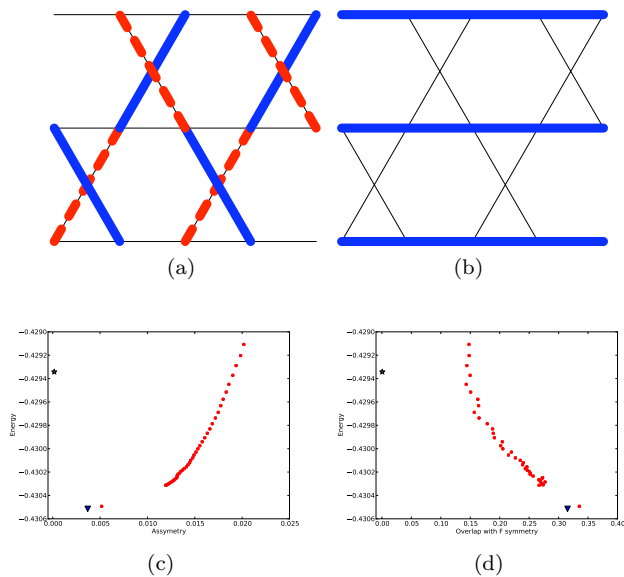


FIG. 3. Spatial symmetry analysis of our state. (a) and (b) are the kagome space group representations associated with the pattern of Fig. 1(b). (c) and (d) Correlation between the energy of different states and the amount of asymmetry ((c): as defined by eqn. 8; (d): as defined by eqn. 9). Red circles correspond to states generated during part of an optimization, the green star to the Dirac spin liquid and the blue triangle to our most optimized state. For energies below the Dirac spin liquid, improved energy is correlated with decreased total asymmetry but increased strength of the F_2 pattern.

although we see a clear symmetry breaking, lower energy states have lower asymmetry, saturating at a value (triangle) that is small but still above the Wen Dirac state (star). We find exactly the opposite behavior for the overlap with the F_2 component: lower energy states have greater overlap. This implies the symmetry breaking associated with the F_2 representation is an important feature of our state throughout much of the minimization process.

In addition to breaking the spatial symmetries of the lattice, the physical system also breaks the $U(1)$ symmetry of the Dirac state down to a Z_2 symmetry. To study this symmetry breaking we produced a series of runs without any pairing in the wave functions. We initialize twelve runs by taking the Dirac pairing function and multiplying each element by $(1+r)$ where r is sampled in the interval $[0, X]$. Using $X = \{0.1, 0.2, 0.33\}$ we ran 12 simulations whose variation in initial energy was significant starting as high as $E = -0.375$ per site. All simulations converged to $E = -0.4295$, the energy of the Dirac state. From these results we conclude that the Dirac state lies at the bottom of a deep and wide region in orbital space and that the pairing of spinons is necessary to produce the state shown in Fig. 1(b).

Based on our results, it seems very likely that the Dirac fixed point is unstable to the formation of a stripe-like

spin-liquid crystal phase. This conclusion rests on two assumptions: that fluctuations beyond those captured by the projected wave function do not restore the symmetry and that this symmetry breaking is not a finite size effect. We have some indirect evidence supporting the latter assumption. DMRG and exact diagonalization results indicate that a 4×4 unit cell cluster should be large enough to capture the qualitative physics of the system. In addition, we have looked at up to 8×8 unit cell clusters and can still find states with lower energy than the Dirac state.

One way to directly address these assumptions would be to perform a PSG analysis on the relevant lower symmetry subgroup of the kagome lattice and use it to search for the state that projects to our state (we cannot do this directly because projection is a many-to-one mapping and cannot be inverted). Such an analysis would allow a determination of the finite size scaling of the symmetry breaking effects and provide a starting point for studying fluctuations about this phase in a low energy effective theory. This would also establish more directly the question of whether there is an energy gap (however, we expect such a gap because the wave vector of the symmetry breaking pattern connects the Dirac nodes of the Brillouin zone).

Given the lack of evidence in large-scale DMRG calculations for our state, it is unlikely to represent the true ground state. However, since it lies very close by and involves a minimal loss of crystal symmetries, it seems likely to be a leading instability. In particular, small perturbations to the Hamiltonian could stabilize it suggesting it could be realized in nature. One promising class of materials are the Zn-Paratacamite family parameterized by Zn doping concentration x with $x < 1/3$. Unlike the structurally perfect kagome lattice of the $x = 1$ Herbertsmithite member of the family, compounds with $x < 1/3$, including clinoatacamite at $x = 0$, break crystal symmetries and have distorted kagome layers[17] with precisely the distortion expected from the symmetry breaking of our state. Our results therefore motivate the study of single crystals of these materials and suggests that either the mysterious intermediate phase below $7\text{K} < T < 20\text{K}$ or the high temperature phase $T > 20\text{K}$ could still have spinons as low energy excitations that are delocalized along the “rails” of the distorted lattice.

The most remarkable implication of our results is its suggestion that spin liquid crystal phases may be a common phenomena. Since any dimer state is the exact ground state at the mean field level[21], projection must introduce quantum fluctuations that melt such crystalline phases, take the system through a succession of more symmetric phases until, in our case, it nearly reaches an isotropic phase. Such a picture has several implications for the DMRG calculations on the kagome lattice. It is known[5] that small perturbations to the Hamiltonian in DMRG (boundary conditions, pinning

fields, etc.) can enhance different states and lead to symmetry breaking. Exploring the class of perturbations that stabilize the symmetry breaking we observe here would help make a deeper connection between analytic Schwinger-fermion theory and DMRG. More interestingly, the observed DMRG state might be understood as a further instability of our state to a nematic spin liquid crystal, a state found recently on a triangular lattice model with ring exchange[22]. A nematic spin liquid phase would be indistinguishable from a spin liquid phase on long cylinders that explicitly break rotational symmetry. Of course, it is also possible that such a putative nematic state melts into an isotropic Z_2 spin liquid. More generically, our results suggest that spin liquid crystal states are common in frustrated antiferromagnets and may be found using methods similar to ours as competitive ground states in many other systems.

ACKNOWLEDGEMENTS

We acknowledge useful discussions with David Huse and Nandini Trivedi. This work used the Extreme Science and Engineering Discovery Environment (XSEDE), which is supported by National Science Foundation grant number OCI-1053575 and the High Performance Computing Cluster at Case Western Reserve University.

[1] M. Hastings, Physical Review B **63**, 1 (2000).

[2] M. Hermele, T. Senthil, and M. P. a. Fisher, Physical Review B **72**, 1 (2005).

- [3] Y. Ran, M. Hermele, P. A. Lee, and X.-G. Wen, Physical Review Letters **98**, 117205 (2007).
- [4] M. Hermele, Y. Ran, P. Lee, and X.-G. Wen, Physical Review B **77**, 224413 (2008).
- [5] S. Yan, D. a. Huse, and S. R. White, Science (New York, N.Y.) **332**, 1173 (2011).
- [6] A. Chubukov, Phys. Rev. Lett. **69**, 832 (1992).
- [7] J. B. Marston and C. Zeng, J. Appl. Phys **69**, 5962 (1991).
- [8] L. Messio, B. Bernu, and C. Lhuillier, “The kagome antiferromagnet: a chiral topological spin liquid?” Unpublished, see arXiv:1110.5440.
- [9] S. Sachdev, Physical Review B **45**, 12377 (1992).
- [10] Y.-m. Lu, Y. Ran, and P. Lee, Physical Review B **83**, 12 (2011).
- [11] F. Nogueira and H. Kleinert, Physical Review Letters **95**, 1 (2005).
- [12] Y. Iqbal, F. Becca, and D. Poilblanc, Physical Review B **83**, 2 (2011).
- [13] S. Depenbrock, I. P. McCulloch, and U. Schollwck, Phys. Rev. Lett. **109**, 067201 (2012).
- [14] H.-C. Jiang, Z. Wang, and L. Balents, “Identifying topological order by entanglement entropy,” Unpublished, see arXiv:1205.4289.
- [15] E. Neuscamman, C. J. Umrigar, and G. K.-L. Chan, Phys. Rev. B **85**, 045103 (2012).
- [16] B. K. Clark, D. A. Abanin, and S. L. Sondhi, Phys. Rev. Lett. **107**, 087204 (2011).
- [17] S.-H. Lee, H. Kikuchi, Y. Qiu, B. Lake, Q. Huang, K. Habicht, and K. Kiefer, Nature Materials **6**, 853 (2007).
- [18] X.-G. Wen, Physical Review B **65** (2002).
- [19] O. Ma and J. B. Marston, Phys. Rev. Lett..
- [20] X.-G. Wen, (Oxford University Press, 2004).
- [21] D. S. Rokhsar, Phys. Rev. B **42**, 2526 (1990).
- [22] T. Grover, N. trivedi, T. Senthil, and P. Lee, Phys. Rev. B **81**, 245121 (2010).